EBioMedicine 13 (2016) 90–98

Contents lists available at ScienceDirect

EBioMedicine

journal homepage: www.ebiomedicine.com

Research Paper

Non-NAD-Like poly(ADP-Ribose) Polymerase-1 Inhibitors effectively Eliminate Cancer *in vivo*

Colin Thomas, Yingbiao Ji, Niraj Lodhi, Elena Kotova, Aaron Dan Pinnola, Konstantin Golovine, Peter Makhov, Kate Pechenkina, Vladimir Kolenko, Alexei V. Tulin *

Fox Chase Cancer Center, Philadelphia, PA, United States

ARTICLE INFO

Article history:
Received 29 August 2016
Received in revised form 3 October 2016
Accepted 3 October 2016
Available online 4 October 2016

Keywords:
PARP-1
PARP-1 inhibitors
Histone-dependent PARP-1 regulation
Poly(ADP-ribose)
Cancer cells

ABSTRACT

The clinical potential of PARP-1 inhibitors has been recognized >10 years ago, prompting intensive research on their pharmacological application in several branches of medicine, particularly in oncology. However, natural or acquired resistance of tumors to known PARP-1 inhibitors poses a serious problem for their clinical implementation. Present study aims to reignite clinical interest to PARP-1 inhibitors by introducing a new method of identifying highly potent inhibitors and presenting the largest known collection of structurally diverse inhibitors. The majority of PARP-1 inhibitors known to date have been developed as NAD competitors. NAD is utilized by many enzymes other than PARP-1, resulting in a trade-off trap between their specificity and efficacy. To circumvent this problem, we have developed a new strategy to blindly screen a small molecule library for PARP-1 inhibitors by targeting a highly specific rout of its activation. Based on this screen, we present a collection of PARP-1 inhibitors and provide their structural classification. In addition to compounds that show structural similarity to NAD or known PARP-1 inhibitors, the screen identified structurally new non-NAD-like inhibitors that block PARP-1 activity in cancer cells with greater efficacy and potency than classical PARP-1 inhibitors currently used in clinic. These non-NAD-like PARP-1 inhibitors are effective against several types of human cancer xenografts, including kidney, prostate, and breast tumors *in vivo*. Our pre-clinical testing of these inhibitors using laboratory animals has established a strong foundation for advancing the new inhibitors to clinical trials.

1. Introduction

Poly(ADP-ribose) polymerase 1 (PARP-1) is an abundant and ubiquitous nuclear enzyme. When active, it captures NAD+ to assemble long and branching polymers of Poly(ADP-ribose) (pADPr), modifying itself, as well as surrounding proteins (D'Amours et al., 1999). Although DNA repair is commonly accepted as its main function, recent findings indicate that PARP-1 also participates in numerous nuclear processes, including regulation of chromatin and gene expression, ribosome biogenesis, nuclear traffic, and epigenetic bookmarking (Krishnakumar et al., 2008; Thomas & Tulin, 2013). PARP-1 tends to control the expression of genes involved in cell adhesion and cell-to-cell signaling (Krishnakumar et al., 2008). Given the multitude of PARP-1 functions, inhibitors of PARP-1 hold promise for several branches of medicine. Preclinical data have shown that PARP-1 inhibitors may mitigate inflammation, circulatory shock, stroke, and myocardial infarction (Curtin & Szabo, 2013). The most extensive research on PARP-1 inhibitors has been carried out in oncology (Alberts, 2009; Curtin, 2005). PARP-1 inhibitors have been shown to selectively eliminate several types of tumorigenic cells, namely BRCA1/2-deficient breast and ovarian cells (Bryant et al., 2005). Indeed, one PARP-1 inhibitor (Olaparib/Lynparza ™, AstraZeneca) has been approved by both the European Medicines Agency and FDA to treat advanced ovarian cancer with BRCA1/2 mutations (Brown et al., 2016) Several PARP-1 inhibitors are currently undergoing phase II/III clinical trials in cancers with or without genetic predisposition, as a monotherapy or in combination with other drugs (Brown et al., 2016). Therefore, PARP-1 inhibitors have already been shown to have the potential required to treat a variety of cancer types, including prostate, colorectal and pancreatic tumors, beyond BRCA1/2 ovarian cancer (Brown et al., 2016; Deshmukh & Qiu, 2015; Lupo & Trusolino, 1846). Unfortunately, a number of clinical studies reported setbacks in research on PARP-1-based anticancer therapies (Guha, 2011). One of the most disappointing studies thus far was the phase III trial of iniparib with gemcitabine and carboplatin in metastatic triple-negative breast cancer (O'Shaughnessy et al., 2014).

The majority of currently available PARP-1 inhibitors (Supplementary Table 1) were designed as NAD competitors and generally represent various memes of nicotinamide pharmacophore (Fig. 1A,B) (Jayle & Curtin, 2011). Ubiquity of NAD in a cell makes it difficult to completely

* Corresponding author at: Cancer Biology Program, Fox Chase Cancer Center, 333 Cottman Avenue, Philadelphia, PA 19111, United States.
E-mail address: Alexei.Tulin@fccc.edu (A.V. Tulin).

http://dx.doi.org/10.1016/j.ebiom.2016.10.001

eliminate PARP-1 activity by using NAD competitors. Specificity of these inhibitors to PARP-1 has been tested and confirmed within the PARP superfamily (Wahlberg et al., 2012). However, little is known about their effect on other NAD-dependent pathways. Since classical PARP-1 inhibitors display strong structural similarities to nucleotides, they tend to obstruct functions of other enzymes that utilize nucleotides as cofactors, such as kinases (Chuang et al., 2012; Antolín et al., 2012; Antolin & Mestres, 2014; Passeri et al., 2015).

To overcome the limitation of NAD-like PARP-1 inhibitors, we set out to identify molecules that inhibit PARP-1, but maintain structural independence from NAD (Tulin, 2011). To accomplish this, we employed a blind screen of a random small- molecule collection containing 50,000 compounds. As noted above, PARP-1 can be regulated by competing for binding with NAD (D'Amours et al., 1999), as well as by two additional routes: obstruction of PARP-1 binding with DNA (Kirsanov et al., 2014) and disruption of PARP-1 interaction with histone H4 (Pinnola et al., 2007). The latter rout of activation is highly specific to PARP-1. Instead of targeting NAD-binding to PARP-1, we searched for molecules that could disrupt PARP-1 activation by the core histone H4 (Fig. 1C). H4-dependent PARP-1 activation is stronger and better sustained than DNA-dependent activation (Fig. 1D). Thus, we designed a new automated approach to screen a large collection of small molecules, using the H4-dependent route. Besides identifying NAD competitors, our screen has identified molecules that show no similarity to NAD, other nucleotides, or to any known PARP-1 inhibitor. Further testing of a subset of these compounds demonstrated their efficacy toward PARP-1 inhibition in cancer cells, as well as their ability to suppress tumorigenesis in prostate and kidney cancer with greater efficacy when compared to current clinically approved drugs and the NAD-competitor Olaparib.

2. Materials and Methods

2.1. Library Screening

An ELISA-like assay developed in our laboratory and tested on the ICCB Library of known substances was used to screen a ChemDiv library of 50,000 small-molecule compounds. The conditions for screening were based on a published protocol (Antolin & Mestres, 2014). DMSO was used as a negative hit control for this screening, and 3AB (known PARP-1 inhibitor) was used as a positive hit control (40 mM concentration as a weak positive control; 400 mM concentration as a strong positive control). Positions of negative controls on a 384-well plate are were as follows: columns 1 and 2: rows A, B, G, H, M and N; columns 23 and 24: rows C, D, I, J, O and P. Positions of weak positive controls on a 384-well plate were as follows: columns 1 and 2: rows C, D, I, J; columns 23 and 24: rows G, H, M, N. Positions of strong positive controls on a 384-well plate were as follows: columns 1 and 2: rows E, F, K, L, O, P; columns 23 and 24: rows A, B, E, F, K, L (Fig. 1F).

Nunc® MaxiSorp™ 384 well plates were coated with histone H4 (3 ng/well) diluted in PBS overnight at RT. Next morning, the plates were washed with PBS-T and blocked with 5% non-fat milk in PBS-T for 1 h at RT. NAD+ solution (260 pMol/well) was distributed to each well, and library compounds and controls were then added to the plates (Fig. 1F). PARP1 mix (2×; prepared separately) was then distributed to NAD+/inhibitors-containing wells, plates were incubated at RT for 1 h and washed twice with PBS-T. Plates were then incubated with primary 10H antibodies (1:4000 in PBS-T/milk) and secondary HRP-conjugated goat *anti*-mouse antibodies (1:1500 in PBST/milk) for 1 h each and washed twice after every incubation with PBS-T. Plates were developed with SureBlue reagent, reactions were stopped with Stop solution (1 N HCl), and absorbance was taken by Perkin Elmer Envision Plate Reader at 450 nm.

2.2. Small-Molecule Clustering Methods

Inhibitor molecules were imported in SMILES format using Canvas, ver. 1.6 (Canvas, 2013). Binary hashed fingerprints were calculated from the 2D structure using a dendritic methodology (Duan et al., 2010). These generated fingerprints were then used as the basis for clustering inhibitors by two methods. The first utilized hierarchical clustering with a Tanimoto similarity metric, and a Schrödinger cluster linkage method yielded 22 clusters by default. Alteration of the merging distance parameter in the resulting dendrogram from 0.96 to 0.9 yielded 96 clusters. The second clustering methodology involved self-organizing maps calculated according to the sum of fingerprint distances to 27 known PARP inhibitors. Molecules were parsed into a 10×10 grid according to this self-organizing approach, measuring similarity to known inhibitors. Twenty-seven individual heat maps of the 10×10 grid showing distance to individual inhibitors were output for comparison.

2.3. Fluorescence of NADH assay

Fluorescence of NADH assay was used to monitor the effect of Olaparib and non-NAD-like inhibitor (5F02) on inhibition of IMPDH activity. IMPDH (Inosine-5′-monophosphate dehydrogenase) catalyzes inosine monophosphate (IMP) with NAD+ as a cofactor to produce Xanthosine monophosphate (XMP) and NADH. The reaction mixture includes 3 μM IMP (Sigma), 5 mM NAD, and 1 μg/μl Recombinant His-tagged human IMPDH2 enzyme (a gift from Dr. Jeffrey R. Peterson of Fox Chase Cancer Center) with/without Olaparib (2 mM) or 5F02 (2 mM) in 100 μl of 1× reaction buffer (100 mm Tris-HCl, pH 7.5; 200 mM KCl; 20 mM MgCl2) at 37 °C. NADH concentration was measured with 340 nm as excitation wavelength and 440 nm as emission wavelength for 10 min using the Cary Eclipse fluorescence spectrophotometer. The reaction rate was plotted based on an established standard curve and converted to the specificity activity of IMPDH (uM NADH/min/mg). The reaction with or without PARP-1 inhibitors was repeated five times. The average value was used for statistical analysis with Student *t*-test.

2.4. Human Cell Cultures

Normal human mammary epithelial cells (HMEC) and Human breast carcinoma cell line BT474 (Lasfargues et al., 1978) were obtained from the Matthew Robinson Lab at Fox Chase Cancer Center and cultured in RPMI 1640 with 10% FBS, sodium pyruvate (10 mM), N-2-hydroxyethylpiperazine-N′-2-ethanesulfonic acid (10 mM) and antibiotics. Androgen-independent human PC-3 prostate cancer cells (Teper et al., 2012) were obtained from ATCC (Rockville, MD). Cells were cultured in RPMI 1640 (Bio-Whittaker, Walkersville, MD) supplemented with 10% FBS (Hyclone, Logan, UT), penicillin (100 μ/ml), streptomycin (100 μg/ml), sodium pyruvate (1 mM) and non-essential amino acids (0.1 mM) under conditions indicated in the figure legends. The renal carcinoma cell (PNX) line (RCC) was a kind gift from Dr. Igor Astsaturov (Fox Chase Cancer Center, Philadelphia, PA). RCC tumor cells were isolated from tumor tissue specimen obtained with written informed consent and Fox Chase Cancer Center Institutional Review Board approval (IRB approved protocol #12–822) from a patient undergoing tumor resection at the Fox Chase Cancer Center.

2.5. PARP-1 Inhibitory Assay in Human Cell Culture

Different doses of new non-NAD-like PARP-1 inhibitors or classical PARP-1 inhibitors 4ANI and PJ34 were added to the cells cultured in complete medium. After 24 or 48 h, cells were lysed, and protein samples were analyzed with SDS-PAGE and Western Blot using *anti*-pADPr antibody.

2.6. Cell Proliferation Assay

Normal cells (HMEC) and breast cancer-derived cells (BT474) were plated at a density of 104 cells/well (100 μl) in a 96-well plate. On the next day, Olaparib, a NAD-mimetic, or new non-NAD-like inhibitors (5F02, 4D11, 5A03, 5H03, 1C09) were added (5 μM). Control cells were grown with DMSO solution added. Cells were grown for 72 h. 20 μl/well of Alamar Blue Reagent were added; fluorescence readings were taken.

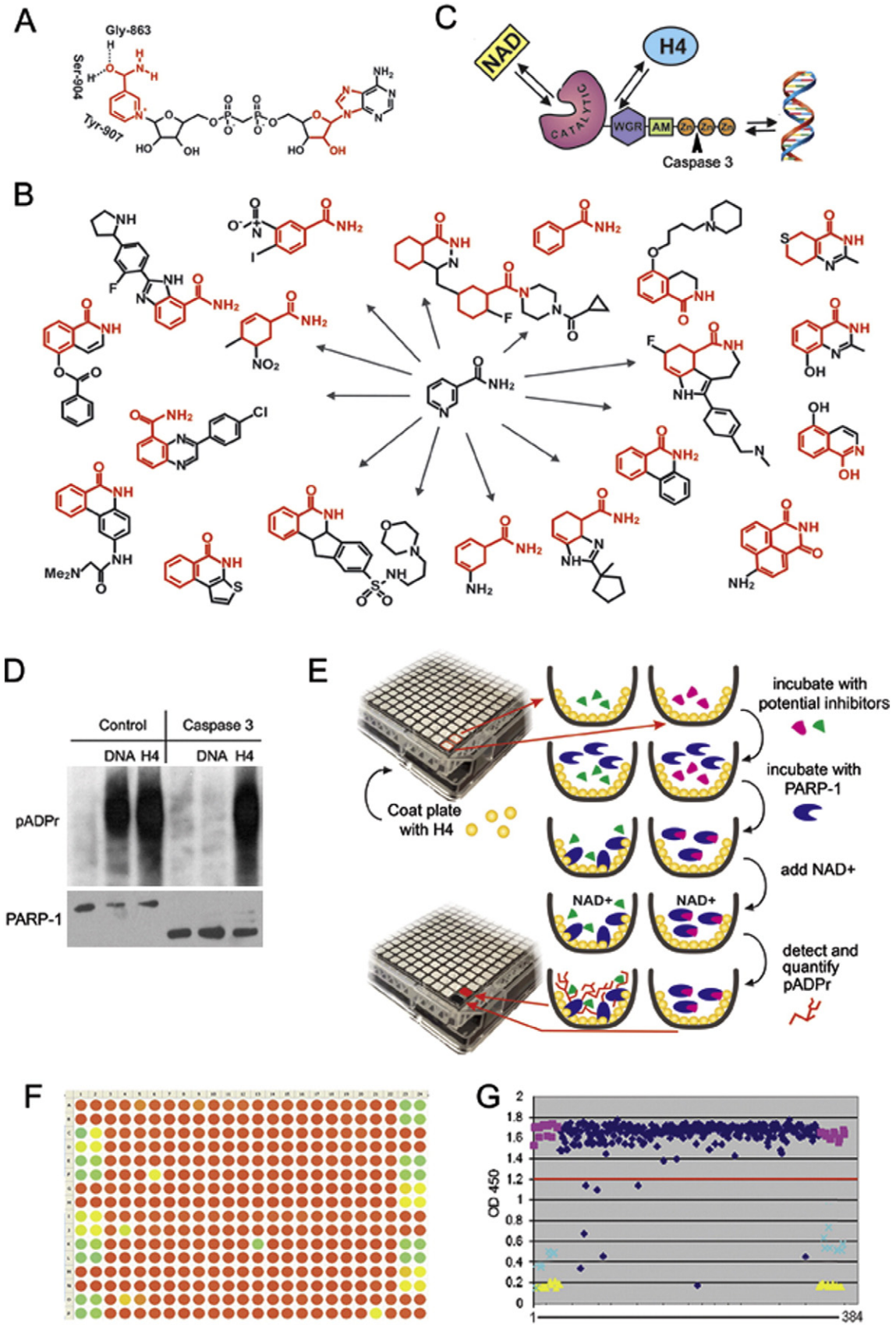

2.7. Clonogenic Cell Survival Assay

The assay was based on a published protocol (Mori et al., 2009). Cells were plated into 24-well plates at a density of 2000 cells/well. Cells were allowed to adhere overnight at 37 °C and treated with increasing concentrations of non-NAD-like PARP-1 inhibitors or classical PARP-1 inhibitor, Olaparib, for 14 days. Colonies were fixed with 70% ethanol for 10 min and stained with 0.25% methylene blue in 30% ethanol for 10 min. After that, staining solution was removed, and plates were rinsed with water. Colonies consisting of 50 cells or more were counted. Data were fitted to exponential and logarithmic decay models using the nonlinear curve fitting module of Statistica 7.0 software. The best fitting models for each inhibitor are represented on the chart. Plating efficiencies (PE) were calculated as follows: PE = number of colonies / number of cells seeded. The surviving fraction (SF) was calculated as follows: SF = number of colonies / number of cells seeded × PE.

2.8. Test of PARP-1 Inhibitors with Xenograft Tumor Models

Ectopic PC-3 or RCC xenograft tumors were established in 6-week-old male C·B17/Icr-scid mice. Animals were treated intraperitoneally with non-NAD-like inhibitor 5F02 (23 mg/kg), classical PARP-1 inhibitor Olaparib (Olap) (50 mg/kg), docetaxel (i.v. 12.5 mg/kg) for prostate xenografts, and the multi-targeted tyrosine kinase inhibitor (TKI) sunitinib (i.v. 40 mg/kg) for RCC xenograft tumors or vehicle (PBS) 5 days a week.

2.9. Assessment of In Vivo Triple-Negative Breast Cancer Tumor Growth

Ectopic xenograft tumors were established using MDA-MB-436, a triple-negative breast cancer cell line. 2 × 106 cells were subcutaneously injected into the flank region of 6-week-old female NGS mice (NOD.Cg-*Prkdcscid Il2rgtm1Wjl*/SzJ, Jackson Laboratory). All animal procedures were carried out in accordance with the institutional guidelines on animal care and with appropriate institutional certification. Animals were fed an autoclaved AIN-93 M diet (Harlan Teklad, Madison, WI) and water *ad libitum*. Twenty days after the injection of tumor cells, animals were randomly assigned to the control or experimental groups ($n = 5$ mice/group). Animals were treated intravenously (I.V.) with non-NAD-like inhibitor 5F02 (4.5 mg/kg), classical PARP-1 inhibitor Olaparib (Olap) (30 mg/kg) or vehicle (10% 2-hydroxypropyl-β-cyclodextrin, PBS × 1) 3 days a week. Tumors were measured twice weekly, and their volumes were calculated as Volume = 0.52 × (width)2 × length.

2.10. Western Blotting

For semi-quantitative protein analysis, cells were lysed in 1 × SDS sample buffer [25 mM Tris (pH 6.8), 2% 2-mercaptoethanol, 3% SDS, 0.1% bromophenol blue, and 5% glycerol] at 1 × 107 cells/ml and then boiled for 5 min. Proteins were resolved by SDS-PAGE and transferred to i-Blot (Invitrogen). The following antibodies were used: rabbit polyclonal *anti*-PARP-1 (C2–10, Trevigen), anti-alpha-actin (Mouse monoclonal, Sigma, #A5441), anti-pADPr (Mouse monoclonal 10H, Tulip, #1020), and either goat anti-rabbit or anti-mouse secondary antibody conjugated to horseradish peroxidase (Sigma). Detection was performed with ECL-Plus (Amersham) and HyBlot CL Autoradiography Film. Image digitizing and quantitative analysis were performed by Odyssey v1.2 software (LI-COR, Lincoln, NE).

2.11. PARP-1 Activity Assay

1 μl of H4-histone (1 μg/μl) or endonuclease-digested plasmid DNA (0.01 μg/μl) was mixed with 25 μl 200 μM NAD and 1 μl of inhibitor/water. This mixture was combined with 10 × PARP-1 reaction buffer (500 mM Tris, pH 8.0, 250 mM MgCl2, 1% Triton X-100) and 0.7 μl PARP-1 enzyme (10 unit/μl, Trevigen). All reactions were carried out for 30 min at room temperature. Samples were examined with SDS-PAGE and Western Blot using *anti*-pADPr antibody.

3. Ethics Statement

This study was carried out in strict accordance with the recommendations from the Guide for the Care and Use of Laboratory Animals, as provided by the American Association of Accreditation of Laboratory Animal Care (AAALAC).

3.1. Statistics

All data are presented as mean ± SEM. Statistical analyses were done using 2-tailed Student's *t*-test. A *P* value of 0.05 or less was considered significant.

4. Results

4.1. Screening Strategy

To establish a screening platform, we designed a PARP-1 activation assay in a 384-well ELISA plate coated with histone H4 protein-activator (Kotova et al., 2011a). PARP-1 reactions were performed in each well in the presence of a single small molecule compound or a positive and a negative control. Accordingly, we were able to detect compounds that could disrupt PARP-1 interaction with the H4 activator, compete with NAD +, or abolish the accumulation of poly (ADP)-ribose, the product of these reactions (Fig. 1E). pADPr was detected as described in (Kotova et al., 2011a). Absorbance at 650 or 450 nm was used as an indicator of PARP-1 activity.

We used the ICCB Known Bioactives Library of 480 compounds, which includes all popular PARP-1 inhibitors, as the test library for our screening. In addition to all known PARP-1 inhibitors, the pilot screening of the test library identified seven molecules previously unknown as PARP-1 inhibitors (Supplementary Table 2). Following the pilot screening, we performed an analysis of 50,000 small compounds, selecting positive hits which significantly reduced PARP-1 activity (Fig. 1F,G). We identified 903 small molecules inhibiting PARP-1 in a cell-free system. After eliminating redundancies that displayed negligible structural differences, we reanalyzed the 639 selected compounds and confirmed that all strong positive hits were 100% reproducible. A total of 373 small molecules in this list inhibited PARP-1 at the same, or better, level than the commonly used PARP-1 inhibitors 4ANI and PJ34.

Fig. 1. Designing a new screening strategy to identify PARP-1 inhibitors. A. PARP-1 binds NAD + by NAD-binding pocket organized by three amino acids, including Gly-863, Ser-904 and Tyr-907, which mostly interact with the nicotinamide part of NAD. The parts of NAD used to develop PARP-1 inhibitors are shown in red. B. Most current PARP-1 inhibitors are developed from nicotinamide pharmacophore. C. Three ways of PARP-1 regulation: 1) competition with NAD for binding, 2) disruption of PARP-1 interaction with histones and 3) obstruction of binding with DNA. Arrowhead shows site of PARP-1 digestion by Caspase 3, which cleaves off DNA binding Zn-fingers of PARP-1, thus abolishing DNA-dependent PARP-1 activation. D. Interaction with the purified core histone H4 activates PARP1 in a DNA-independent manner. Full-length PARP-1 protein (left) and PARP1 protein cleaved by Caspase 3 (right) were preincubated with randomly broken DNA or core histone H4, followed by mixing with NAD. The product of PARP-1 enzymatic activity, poly(ADP-ribose), was detected after PAGE on a Western blot using *anti*-pADPr antibody. These data clearly demonstrate that the DNA-binding domain of PARP1 (Zn-fingers I and II) is not required for histone-dependent PARP1 activation. E. Schematic representation of the pipeline used to identify PARP-1 inhibitors. F-G. Data were visualized in a colour-coded table representing the 384-well plate in which potential inhibitors could be identified as green or yellow circles corresponding to wells that had minimal pADPr signal (F) or on a graph representing relative numerical value of this signal when compared to positive (yellow) or negative (purple) controls (G).

A large number of the newly identified PARP-1 inhibitors demonstrated obvious structural similarities to the known PARP-1 inhibitors. To narrow down the list of small molecules for further analysis, we used a computational approach. First, we sorted out new PARP-1 inhibitors based on the presence of an obvious structural core, similar to known biologically active molecules. We identified 10 subgroups based on this approach (Fig. 2A) (Supplementary Tables 3-1–3-10). Three hundred and forty-four structurally heterogeneous small molecules without obvious homology to known compounds were assigned to 11 subgroups (Supplementary Tables 3-11).

4.2. *N-Methylpiperidin/N-Methylmorpholino/N-Methylpyrrolidine/dipxolanyl Group*

Even without a common structural core molecule, the compounds could expose their epitopes in a manner similar to that of NAD-like PARP-1 inhibitors. To eliminate small molecules that displayed 3D structural similarity to known PARP-1 inhibitors, we used Canvas, ver. 1.6 (Canvas, 2013). This software allowed us to sort out small molecules by the 3D positions of certain epitopes, or fingerprints. Information about the structure of small molecules was imported in SMILES format. We implemented a clustering analysis based on self-organizing maps calculated as the sum of fingerprint distances for all new PARP-1 inhibitors and the 27 known PARP-1 inhibitors and NAD (Supplementary Table 1). This allowed us to sort our collection of 639 molecules and their 3D isomers, as well as the 27 known inhibitors, into a 2D matrix, each cell of which contained similar molecules (Fig. 2B). Thus, greater similarity was detected in neighboring cells, but such similarity decreased with distance. Heat colors were used to represent the degree of similarity in each cell (Fig. 2C). After superimposing these maps, we identified an area of the matrix with no similarity to known PARP-1 inhibitors and NAD (Fig. 2C, red square). This area contains 52 small molecules (Supplementary Table 4), which include a group of 17 structurally related small molecules (Fig. 2D). This subgroup of non-NAD-like PARP-1 inhibitors was tested further.

These non-NAD-like molecules show a strong capacity to inhibit PARP-1 *in vitro*. Structurally, these molecules could be split into two subgroups (Fig. 2D): the first contains the core element 2-(*N*-methylpiperidin-1-yl)acetate or 2-(*N*-methylmorpholino)acetate or 2-(*N*-methylpyrrolidine-1-yl)acetate; the second contains the core element 1-((1,3-dioxolane-4-yl)methyl)piperidine or 1-((1,3-dioxolane-4-yl)methyl)*N*-methylmorpholino or 1-((1,3-dioxolane-4-yl)methyl) *N*-methylpyrrolidine. In addition, two molecules show similarities to the second group in that they also possess dioxolane-4-yl in their structure (Fig. 2D), but they are otherwise structurally quite distinct. These 17 non-NAD-like PARP-1 inhibitors have no obvious structural homologues among components of eukaryotic enzymatic pathways. Therefore, they should have greater efficacy and lower toxicity than classical NAD-like PARP-1 inhibitors.

We confirmed the efficacy of the selected set of new inhibitors using a cell-free activation assay. Unlike the classical PARP-1 inhibitors PJ34, Olaparib and 4ANI, these new inhibitors are very effective in suppressing both DNA- and histone-dependent PARP-1 activation pathways (Supplemental Fig. S1A). Since inhibiting PARP-1 in a cell-free system does not warrant activity of a compound in the cell, we further tested selected compounds for their ability to block PARP-1 in human cells.

We used an inosine-5′-monophosphate dehydrogenase (IMPDH) activity assay (Fig. 2E) to test whether Olaparib and our lead compound, 5F02, compete with NAD to reduce the production of NADH in the IMPDH reaction. Olaparib, as a structural analogue of NAD, decreased IMPDH activity by two-fold, suggesting that Olaparib interferes with metabolic pathways associated with NAD (Fig. 2F). In contrast, 5F02 showed no significant reduction of NADH production in the IMPDH assay (Fig. 2F). This result confirmed that non-NAD-like inhibitors like 5F02 are more specific in their mode of action. Specificity of NAD-like inhibitors to PARP-1 has been tested and confirmed within the PARP superfamily (Wahlberg et al., 2012). Our lead compound 5F02 is also highly specific for PARP-1 inhibition (Supplemental Fig. S1B).

4.3. *New PARP-1 Inhibitors Block PARP-1 Activity and Suppress Tumorigenic Potential of Cancer Cells*

To determine whether the new compounds are capable of inhibiting PARP-1 in a cell-based system, we tested their activity using different human cancer cells. Previously, we found that breast (BT474), prostate (PC3), and kidney (PNX0010) cancer cells show an unusually high level of PARP-1 activity (Kirsanov et al., 2014). Therefore, we used these cell lines to test the efficacy of PARP-1 inhibition by new and classical inhibitors. When we cultured these cells with NAD competitors, either 4ANI or PJ34, the amount of pADPr was considerably diminished (Fig. 3A). Likewise, all 17 molecules identified by our screen showed a similar magnitude of PARP-1 inhibition in human cancer cells (Fig. 3A). Olaparib and non-NAD-like inhibitors effectively suppressed the proliferation of breast cancer-derived cells (Supplemental Fig. S2A). Importantly, however, non-NAD-like inhibitors demonstrated no cytotoxicity to normal cells, while Olaparib suppressed the growth of both normal and cancer cells (Supplemental Fig. S2A). Moreover, our lead compound 5F02 shows no cytotoxicity to any of tested normal cell lines derived from breast, prostate and kidney, while Olaparib significantly repressed the viability of these cells (Supplemental Fig. S2B, C, D).

Since the selected panel of new inhibitors demonstrated no cytotoxicity on normal human cells, we next tested their ability to suppress the malignant potential of tumor-derived cells. Unlike normal cells, cancer-derived cells are capable of establishing colonies growing on TC plates (Maruyama et al., 1975; Cifone & Fidler, 1980; Li et al., 1989). Thus, we employed a colonogenic assay to examine our lead compound, 5F02. We found that 5F02 consistently suppressed colony growth for all tested cell types, while Olaparib was significantly weaker (Fig. 3B–G). Interestingly, when equal doses of 5F02 and Olaparib were administered, we noticed a synergistic, *i.e.*, additive, effect on increased suppression of colony growth (Fig. 3B–G).

To further confirm this synergism, we compared the activity of Olaparib with five new non-NAD-like inhibitors (5F02, 4D11, 5A03, 5H03, 1C09) separately and in combination, using a PC-3 colonogenic assay. Although the effects of each individual new compound on the growth of PC-3 cells varied considerably, all of them suppressed colony

Fig. 2. Identifying non-NAD-like small molecules inhibiting PARP-1 protein. A. Sorting out new PARP-1 inhibitors based on the presence of an obvious structural core, similar to known biologically active molecules. Eleven subgroups were identified. Structural cores and numbers of molecules falling in each group are indicated. B. Sorting out 639 new plus 27 known PARP-1 inhibitors and NAD based on 3D fingerprints, using the Canvas, ver. 1.6, program. Based on similarity of fingerprints, compounds were sorted to a 2D matrix containing 100 cells. The number of small molecules with all their 3D isomers in each cell is indicated. C. Comparison of molecules sorted in the matrix with each known PARP-1 inhibitor and NAD. Similarity is illustrated by heat map. Red corresponds to highest similarity and blue to absence of similarity. Name of inhibitor is indicated above the map. Bottom-right square represents a superimposure of 27 heat maps and reveals the area of matrix (labeled with red border) containing non-NAD-like compounds. D. Molecular structures of new PARP-1 inhibitors. Structural cores: I - 2-(*N*-methylmorpholino) acetate; II - 2-(*N*-methylpiperidin-1-yl)acetate; III - 2-(*N*-methylpyrrolidine-1-yl)acetate; IV - 1-((1,3-dioxolane-4-yl)methyl)*N*-methylmorpholino; V - 1-((1,3-dioxolane-4-yl)methyl) piperidine; VI - 1-((1,3-dioxolane-4-yl)methyl) *N*-methylpyrrolidine. E. Schematic illustration of IMPDH2 catalyzing reaction. F. Non-NAD-like inhibitors do not disrupt IMPDH2 activity. Graph showing IMPDH specific- activity in the IMPDH reaction with/without PARP-1 inhibitors. Column1: no recombinant human IMPDH2 added in the reaction. Column2: human IMPDH2 with 2 ul DMSO in the reaction. Column3: human IMPDH2 with 2 mM Olaparib in the reaction. Column 4: human IMPDH2 with 2 mM 5F02 in the reaction. **: $P < 0.01$.

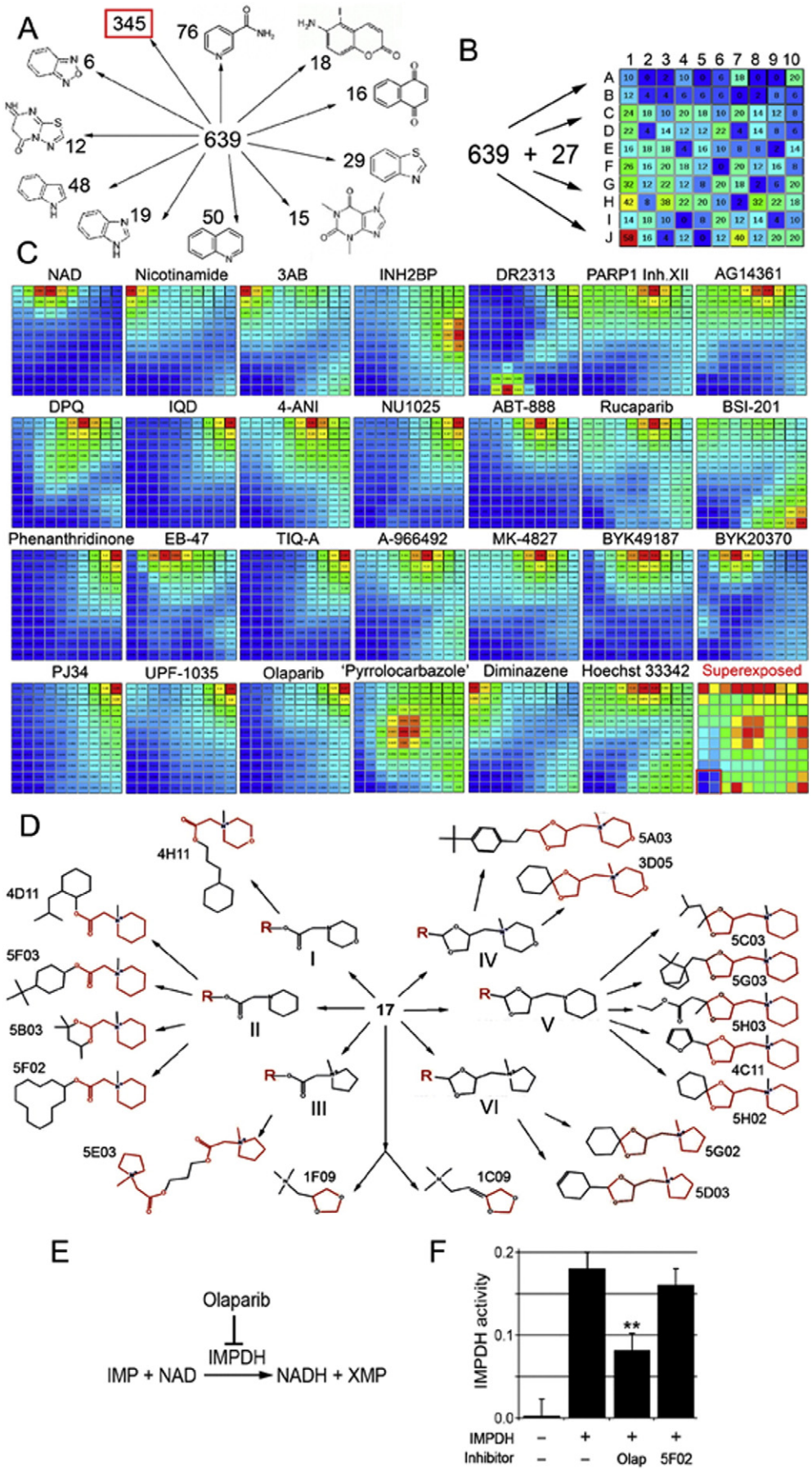
A
345
639
6
76
18
16
12
29
48
19
50
15
B
639 + 27
1 2 3 4 5 6 7 8 9 10
A
B
C
D
C
NAD
Nicotinamide
3AB
INH2BP
DR2313
PARP1 Inh.XII
AG14361
DPQ
IQD
4-ANI
NU1025
ABT-888
Rucaparib
BSI-201
Phenanthridinone
EB-47
TIQ-A
A-966492
MK-4827
BYK49187
BYK20370
PJ34
UPF-1035
Olaparib
'Pyrrolocarbazole'
Diminazene
Hoechst 33342
Superexposed
D
4H11
4D11
5F03
5B03
5F02
5E03
I
II
III
17
IV
V
VI
5A03
3D05
5C03
5G03
5H03
4C11
5H02
5G02
5D03
1F09
1C09
E
Olaparib
IMPDH
IMP + NAD
NADH + XMP
F
IMPDH activity
0.2
0.1
0.0
**
IMPDH
Inhibitor
–
+
+
+
–
–
Olap
5F02

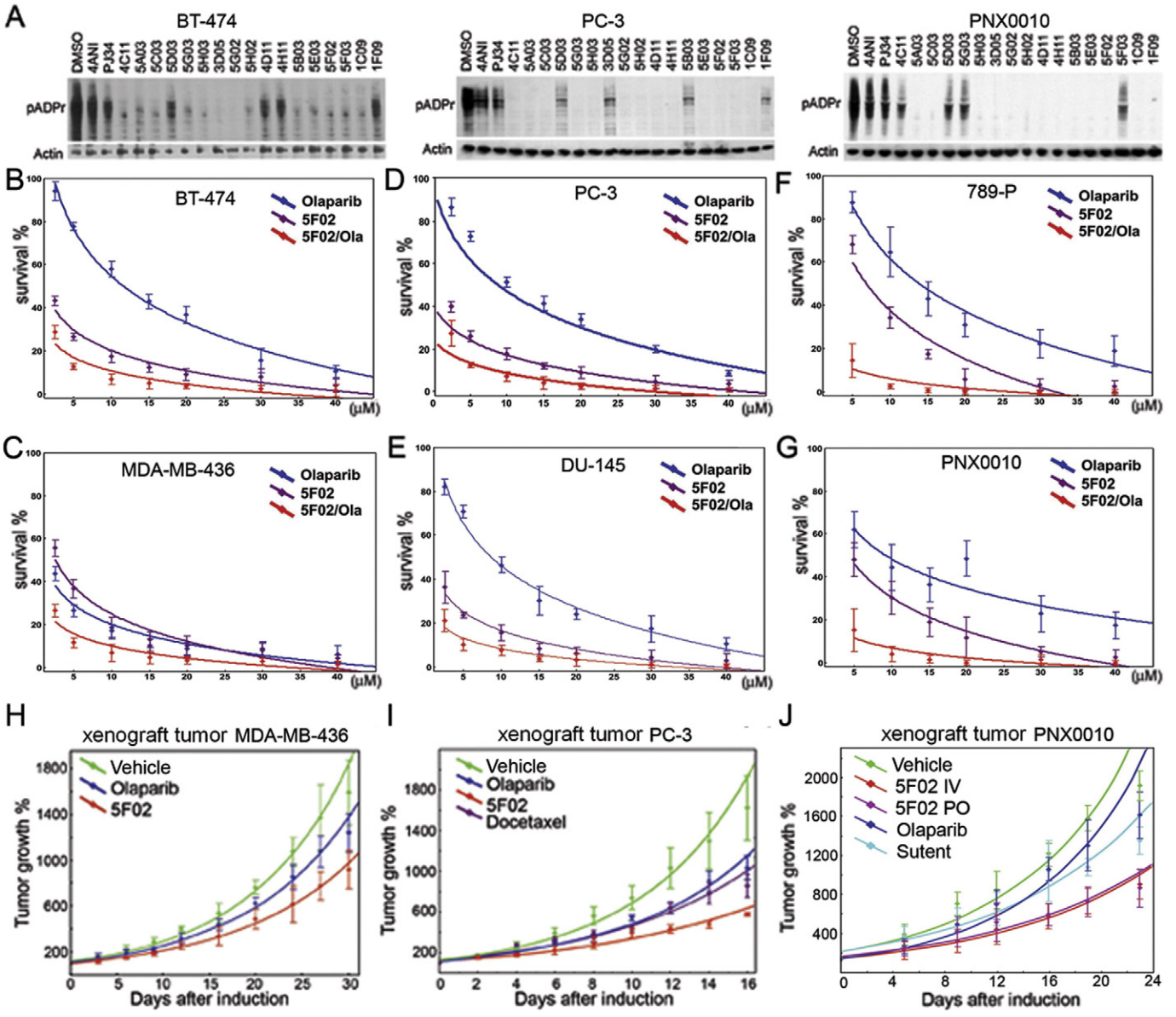

Fig. 3. PARP-1 inhibition and tumor cell suppression by classical NAD-mimetic and novel non-NAD-like PARP-1 inhibitors. (A) Non-NAD-like PARP-1 inhibitors block PARP-1 activity in human cells. A comparative analysis of PARP-1 activity in BT474, PC-3, and RCC cells cultured without and with classical PARP-1 inhibitors, 4ANI or PJ34, and new inhibitors identified in our screen. To detect pADPr on Western blot, we used mAb 10H antibody against pADPr. pAb antibody against Actin was used as a loading control. Reduction of pADPr was detected by Western blotting for inhibitor-treated cells relative to DMSO-treated cells. (B-G) New PARP-1 inhibitors suppress malignancy potential of cancer-derived cells: BT474 (breast cancer) (B); MDA-MB-436 (breast cancer) (C); PC-3 (prostate cancer) (D); DU145 (prostate cancer) (E); 789-P (RCC) (F); PNX0010 (RCC) (G). Calculation of cell survival rate in (B-G) was based on clonogenic cell survival assays. Cells were plated into 24-well plates. Cells were allowed to adhere overnight and were treated with a non-NAD-like inhibitor (5F02) (magenta), Olaparib (blue), and both (red) for 14 days. Colonies were counted and plotted on the graph. Data were fitted to exponential and logarithmic decay models using nonlinear curve fitting module of Statistica 7.0 software. The best fitting models for each inhibitor are represented on the chart. (H-J) Non-NAD-like PARP-1 inhibitors suppress tumor growth *in vivo*. 5F02 inhibitor suppresses growth of triple-negative breast cancer MDA-MB-436 (H), androgen-independent PC-3 (I), and renal cell carcinoma (PNX) (J) xenograft tumors *in vivo*. Ectopic MDA-MB-436 PC-3 or RCC xenograft tumors were established in 6-week-old male C·B17/Icr-scid mice (NOD.Cg-*Prkdc*^{scid} *Il2rg*^{tm1Wjl}/SzJ mice for MDA-MB-436). Animals were treated intraperitoneally with non-NAD-like inhibitor 5F02 (23 mg/kg), classical PARP-1 inhibitor Olaparib (Olap) (50 mg/kg), docetaxel (i.v. 12.5 mg/kg) for prostate xenografts, multi-targeted tyrosine kinase inhibitor (TKI) sunitinib (i.v. 40 mg/kg) for RCC xenograft tumors, or vehicle (PBS) 5 days a week. Values shown represent means ($n = 5$) + SEM. (J) 5F02 suppresses growth of RCC xenograft tumors. Xenograft tumors were established in 6-week-old male C·B17/Icr-scid mice using PNX0010 RCC cells generated from a clinical specimen of kidney cancer resistant to sunitinib treatment. Animals were treated with new PARP-1 inhibitor 5F02 (4 mg/kg intravenously (i.v.) or 6 mg/kg orally (p.o.)), classical PARP-1 inhibitor Olaparib (20 mg/kg, i.v.), sunitinib (40 mg/kg, p.o.), or vehicle 5 days a week. Values shown represent means (n = 5) + SEM. Data were fitted to exponential growth models using nonlinear curve fitting module of Statistica 7.0 software. (H-J) Data were fitted to exponential growth models using nonlinear curve fitting module of Statistica 7.0 software. Error bars correspond to standard deviation based on 5 repeats.

growth with greater efficacy compared to the classical PARP-1 inhibitor Olaparib alone (Supplemental Fig. S2E). Moreover, non-NAD-like inhibitors synergistically enhance the effect of NAD-competitors on the suppression of the growth of colonies (Supplemental Fig. S2F).

In light of encouraging *in vitro* data, we examined the antitumor activity of non-NAD-like inhibitor 5F02, using a triple-negative breast cancer tumor growth *in vivo*. Subcutaneous MDA-MB-436 tumors were established in 6-week-old female NGS mice. Treatment with 5F02 or Olaparib and assessment of tumor growth were performed as described in Materials and Methods. As expected, the classical PARP-1 inhibitor Olaparib slowed down the triple-negative tumor growth. At the same time, 5F02 suppressed tumor growth with a greater efficacy (Fig. 3H).

Next, we compared the effects of Olaparib and 5F02 in castration-resistant androgen receptor-negative PC-3 prostate cancer and PNX0010 renal cell carcinoma (RCC) xenograft animal models. As demonstrated in Figs. 3I and J, animals treated with non-NAD-like inhibitor 5F02 showed a significantly stronger inhibition of tumor growth relative to control animals and animals treated with the classical PARP-1 inhibitor Olaparib. Moreover, non-NAD-like inhibitors demonstrated superior *in vivo* antitumor activity compared with clinically relevant anticancer drugs, *i.e.*, docetaxel (Tannock et al., 2004) for prostate xenografts and multi-targeted tyrosine kinase inhibitor (TKI) sunitinib (Motzer et al., 2007) for RCC xenograft tumors. Importantly, treatment with 5F02 was well tolerated by all animals, with no apparent signs of toxicity.

Finally, we tested the oral bioavailability of 5F02. We compared the ability 5F02 to suppress RCC tumor growth *in vivo* when it was delivered intravenously or orally. The graph presented in Fig. 3J demonstrated that oral delivery of 5F02 (5F02 PO) is as effective as that delivered by the intravenous route (5F02 IV).

5. Discussion

Clinical interest in PARP-1 has increased over the past decade with the recognition of its roles in transcription regulation, DNA repair, epigenetic bookmarking, and chromatin restructuring. Currently, over one hundred clinical studies are being carried out to evaluate PARP-1 inhibitors, most involving oncology (Feng et al., 2015). Given the initial promising results for treating certain types of cancer, the impetus is now focused on finding more effective and less cytotoxic PARP-1 inhibitors.

Whereas the NAD-dependent route of PARP-1 activation has been exhaustively exploited for designing new inhibitors, the other two known routes of activation, namely, the histone H4- and DNA-dependent pathways, remain overlooked. Here we have reported the discovery of new PARP-1 inhibitors using a screen based on PARP-1 enzymatic activation *via* histone H4 (Passeri et al., 2015; Kotova et al., 2011b; Thomas et al., 2014). The screening for compounds inhibiting H4-induced PARP-1 activity also identified molecules similar in structure to NAD, including those acting like previously known PARP-1 inhibitors. Other inhibitors identified by the screen represent a new generation of PARP-1 inhibitors that are not NAD analogues. Because NAD is a crucial metabolic currency within cells, compounds that mimic NAD disrupt multiple cellular processes, leading to off-target effects. Therefore, novel non-NAD-like PARP-1 inhibitors are expected to possess minimal secondary toxicity, as they target an activation mechanism unique to the PARP-1 enzyme.

Notably, the new non-NAD-like PARP-1 inhibitors demonstrate higher efficacy against several types of tumors compared to the classical NAD-like PARP-1 inhibitors. Activation of PARP-1 *via* histone H4 has been best described within the context of transcription regulation and changes in chromatin structure (Kotova et al., 2011b; Thomas et al., 2014). The expanse of histone-mediated PARP-1 activity, however, within the various known functions of PARP-1, *e.g.*, DNA repair, is yet to be fully understood. The mechanism of action of these new- generation PARP-1 inhibitors is not clear and may involve several routes, *e.g.*, obstructing PARP-1 interaction with H4 or provoking an inhibitory conformational change. Inhibiting allosteric regulation of PARP-1 has recently been shown to be another potential approach to the targeting of PARP-1 function (Steffen et al., 2014).

When PARP-1 inhibitors were first evaluated for their potential in treating cancer, the underlying rationale for their application was to prevent PARP-1-mediated DNA repair, thereby reducing the survival potential of carcinogenic cells. Consequently, in oncology, PARP-1 inhibitors have been primarily tested either to increase the efficacy of cytotoxic therapies or as a monotherapy *via* synthetic lethality in tumors with already notable defective DNA repair pathways, namely homologous recombination. The synthetic lethality approach has been most extensively explored in BRCA1/2-deficient ovarian and breast cancers (Feng et al., 2015). The first PARP-1 inhibitor was recently approved by the FDA to treat ovarian cancer in women with BRCA1/2 mutations who had already failed three or more chemotherapy treatments. However, the responses to this therapeutic approach have been dramatically varied in patients with BRCA mutations, even including improved outcomes in cohorts of patients with wild-type BRCA genes (Duan et al., 2010; Ledermann et al., 2012; Ledermann et al., 2014). It has been speculated that PARP-1 inhibitor efficacy in oncology extends into its role in regulating transcription and chromatin structure (Maruyama et al., 1975). Maintaining an active chromatin state for transcribing genes is the central component in rapidly dividing cells (Lodhi et al., 2014), particularly those that are carcinogenic (Krishnakumar et al., 2008). It has also been shown that PARP-1 plays an integral role in transcription regulation of hormone-dependent cancers (Schiewer & Knudsen, 2014; Brenner et al., 2011). Overall, it seems clear that the role of PARP-1 inhibitors in oncology extends beyond initial experiments that targeted the role of PARPs in DNA repair.

Apart from oncology, preclinical efficacy of PARP-1 inhibitors in mitigating inflammation, circulatory shock, myocardial infarction, and stroke likely results from the inhibition of PARP-1-mediated transcription activation (Curtin & Szabo, 2013). It has been shown that transcriptional profiles are dramatically altered by PARP-1 inhibition in innate immune signaling pathways, potentially dampening aberrant inflammatory activation (Gupte et al., 2015). So far, the introduction of these inhibitors beyond oncology has been hampered by the possible risks of toxicity and carcinogenesis, secondary to inhibiting an integral component of DNA repair (Maruyama et al., 1975). Therefore, finding inhibitors that are less cytotoxic and more selective toward PARP-1-mediated transcription would be of considerable clinical interest. However, the extent of PARP-1-mediated transcription in DNA repair is not entirely clear. Although it cannot be determined at this time whether these new inhibitors have a stronger predilection toward targeting PARP-1-mediated transcription, their antitumor potential and significant reduction in cytotoxicity could launch PARP-1 inhibitors further into other areas of molecular medicine.

Funding

This research was supported by grants from the National Institutes of Health (R01 GM077452 and R01 DK082623) to A.V.T. The costs incurred for purchasing the subcollection of new PARP-1 inhibitors were partially covered by the Kahn's family gift to A.V.T. Funding agencies had no role in study design, data collection, data analysis, interpretation, writing of the report.

Conflict of Interest

We have no conflicts of interest with regard to the subject of this paper.

Author Contributions

AVT, EK, and ADP conceived and designed the screen approaches; EK performed screens and initial data analysis; CT, YJ, NL, and DP performed the Western blot analysis; CT, NL, EK, KG, and PM performed cell proliferation and clonogenic cell survival assays; PM and VK designed and performed experiments with xenograft tumor models. KP performed the statistical analysis; CT, KP, and AVT wrote the manuscript.

Acknowledgments

We thank Drs. M. Robinson, N. Johnson, and I. Astaturov for providing human cancer-derived cells. Drs. K. Zaret and N. Johnson, as well as Mr. D. Martin, provided comments on the earlier versions of the manuscript. Screening for new PARP-1 inhibitors was performed in the

Transnational Facility at FCCC. The molecular modeling analysis was performed in the FCCC Molecular Modeling Facility. The large amount of the lead compound 5F02 was synthesized in the Organic Synthesis Facility at FCCC by Dr. C.B. Myers. We are also grateful to Dr. J. Peterson for his help with setting up the IMPDH activity assay in our lab.

Appendix A. Supplementary data

Supplementary data to this article can be found online at http://dx.doi.org/10.1016/j.ebiom.2016.10.001.

References

Alberts, B., 2009. Redefining cancer research. Science 325, 1319.
Antolin, A.A., Mestres, J., 2014. Linking off-target kinase pharmacology to the differential cellular effects observed among PARP inhibitors. Oncotarget 5, 3023–3028.
Antolín, A.A., Jalencas, X., Yélamos, J., Mestres, J., 2012. Identification of pim kinases as novel targets for PJ34 with confounding effects in PARP biology. ACS Chem. Biol. 7, 1962–1967.
Brenner, J.C., Ateeq, B., Li, Y., Yocum, A.K., Cao, Q., Asangani, I.A., et al., 2011. Mechanistic rationale for inhibition of poly(ADP-ribose) polymerase in ETS gene fusion-positive prostate cancer. Cancer Cell 19, 664–678.
Brown, J.S., Kaye, S.B., Yap, T.A., 2016. PARP inhibitors: the race is on. Br. J. Cancer 114, 713–715.
Bryant, H.E., Schultz, N., Thomas, H.D., Parker, K.M., Flower, D., Lopez, E., et al., 2005. Specific killing of BRCA2-deficient tumours with inhibitors of poly (ADP-ribose) polymerase. Nature 434, 913–917.
Canvas, 2013. Version 1.6. Schrödinger, LLC, New York, NY.
Chuang, H.C., Kapuriya, N., Kulp, S.K., Chen, C.S., Shapiro, C.L., 2012. Differential anti-proliferative activities of poly (ADP-ribose) polymerase (PARP) inhibitors in triple-negative breast cancer cells. Breast Cancer Res. Treat. 134, 649–659.
Cifone, M.A., Fidler, I.J., 1980. Correlation of patterns of anchorage-independent growth with in vivo behavior of cells from a murine fibrosarcoma. Proc. Natl. Acad. Sci. 77, 1039–1043.
Curtin, N.J., 2005. PARP inhibitors for cancer therapy. Expert Rev. Mol. Med. 7, 1–20.
Curtin, N.J., Szabo, C., 2013. Therapeutic applications of PARP inhibitors: anticancer therapy and beyond. Mol. Asp. Med. 34, 1217–1256.
D'Amours, D., Desnoyers, D., Dsilva, I., Poirier, G., 1999. Poly(ADP-ribosyl)ation reactions in the regulation of nuclear functions. Biochem. J. 342, 249–268.
Deshmukh, D., Qiu, Y., 2015. Role of PARP-1 in prostate cancer. American journal of clinical and experimental urology 3, 1–12.
Duan, J., Dixon, S.L., Lowrie, J.F., Sherman, W., 2010. Analysis and comparison of 2D fingerprints: insights into database screening performance using eight fingerprint methods. J. Molec. Graph. Model. 29, 157–170.
Feng, F., Bono, J., Rubin, M., Knudsen, K., 2015. Chromatin to clinic: the molecular rationale for PARP1 inhibitor function. Mol. Cell 58, 925–934.
Guha, M., 2011. PARP inhibitors stumble in breast cancer. Nat. Biotechnol. 29, 373–374.
Gupte, R., Nandu, T.S., Kraus, W.L., 2015. Role of PARP-1 in modulating pro-inflammatory signaling in macrophages. Endocr. Rev. 36.
Jayle, M., Curtin, N.J., 2011. The potential for poly (ADP-ribose) polymerase inhibitors in cancer therapy Ther. Adv. Med. Oncol. 3, 257–267.
Kirsanov, K.I., Kotova, E., Makhov, P., Golovine, K., Lesovaya, E.A., Kolenko, V.M., et al., 2014. Minor grove binding ligands disrupt PARP-1 activation pathways. Oncotarget 5, 428–437.
Kotova, E., Lodhi, N., Jarnik, M., Pinnola, A.D., Ji, Y., Tulin, A.V., 2011b. Drosophila histone H2A variant (H2Av) controls poly(ADP-ribose) polymerase 1 (PARP1) activation in chromatin. Proc. Natl. Acad. Sci. 15, 6205–6210.
Kotova, E., Pinnola, A.D., Tulin, A.V., 2011a. Small-molecule collection and high-throughput Colorimetic assay to identify PARP-1 inhibitors. Methods Mol. Biol. 780, 491–516.
Krishnakumar, R., Gamble, M.J., Frizzell, K.M., Berrocal, J.G., Kininis, M., Kraus, W.L., 2008. Reciprocal binding of PARP-1 and histone H1 at promoters specifies transcriptional outcomes. Science 319, 819–821.
Lasfargues, E.Y., Coutinho, W.G., Redfield, E.S., 1978. Isolation of two human tumor epithelial cell lines from solid breast carcinomas. J. Natl. Cancer Inst. 61, 967–978.
Ledermann, J., Harter, P., Gourley, C., Friedlander, M., Vergote, I., Rustin, G., et al., 2014. Olaparib maintenance therapy in patients with platinum-sensitive relapsed serous ovarian cancer: a preplanned retrospective analysis of outcomes by BRCA status in a randomized phase 2 trial. Lancet Oncol. 15, 852–861.
Ledermann, J., Harter, P., Gourley, C., Friedlander, M., Vergote, M.I., Rustin, G., et al., 2012. Olaparib maintenance therapy in platinum-sensitive relapsed ovarian cancer. N. Engl. J. Med. 366, 1382–1392.
Li, L., Price, J.E., Fan, D., Zhang, R.D., Bucana, C.D., Fidler, I.J., 1989. Correlation of growth capacity of human tumor cells in hard agarose with their in vivo proliferative capacity at specific metastatic sites. J. Natl. Cancer Inst. 81, 1406–1412.
Lodhi, N., Kossenkov, K.V., Tulin, A.V., 2014. Bookmarking promoters in mitotic chromatin: poly(ADP-ribose)polymerase-1 as an epigenetic mark. Nucleic Acids Res. 42, 7028–7038.
Lupo, B., Trusolino, L., 2014. Inhibition of poly (ADP-ribosyl) ation in cancer: old and new paradigms revisited. Biochimica et Biophysica Acta (BBA)-Reviews on Cancer 1846 201–215.
Maruyama, K., East, J.L., Wagner, S.H., Dmochowski, L., 1975. In vitro transformation of cells from human neoplasms. Bibl. Haematol. 40, 85–92.
Mori, S., Chang, J.T., Andrechek, E.R., Matsumura, N., Baba, T., Yao, G., et al., 2009. Anchorage-independent cell growth signature identifies tumors with metastatic potential. Oncogene 28, 2796–2805.
Motzer, R., Hutson, T.E., Tomczak, P., Michaelson, M.D., Bukowski, R.M., Rixe, O., et al., 2007. Sunitinib versus interferon alpha in metastatic renal-cell carcinoma. N. Engl. J. Med. 356, 115–124.
O'Shaughnessy, J., Schwartzberg, L., Danso, M.A., Miller, K.D., Rugo, H.S., Neubauer, M., et al., 2014. Phase III study of iniparib plus gemcitabine and carboplatin versus gemcitabine and carboplatin in patients with metastatic triple-negative breast cancer. J. Clin. Oncol. 32, 3840–3847.
Passeri, D., Camaioni, E., Liscio, P., Sabbatini, P., Ferri, M., Carotti, A., Giacchè, N., Pellicciari, R., Gioiello, A., Macchiarulo, A., 2015. Concepts and molecular aspects in the Polypharmacology of PARP-1 inhibitors. ChemMedChem http://dx.doi.org/10.1002/cmdc.201500391.
Pinnola, A., Naumova, N., Shah, M., Tulin, A.V., 2007. Nucleosomal core histones mediate dynamic regulation of poly(ADP-ribose) polymerase 1 protein binding to chromatin and induction of its enzymatic activity. J. Biol. Chem. 44, 32511–32519.
Schiewer, M.J., Knudsen, K.E., 2014. Transcriptional roles of PARP1 in cancer. Mol. Cancer Res. 12, 1069–1080.
Steffen, J.D., Tholey, R.M., Langelier, M.F., Planck, J.L., Schiewer, M.J., Lal, S., et al., 2014. Targeting PARP-1 allosteric regulation offers therapeutic potential against cancer. Cancer Res. 74, 31–37.
Tannock, I., de Wit, R., Berry, W.R., Horti, J., Pluzanska, A., Chi, K.N., et al., 2004. Docetaxel plus prednisone or mitoxantrone plus prednisone for advanced prostate cancer. N. Engl. J. Med. 351, 1502–1512.
Teper, E., Makhov, P., Golovine, K., Canter, D.J., Myers, C.B., Kutikov, A., et al., 2012. The effect of 5-aminolevulinic acid and its derivatives on protoporphyrin IX accumulation and apoptotic cell death in castrate-resistant prostate cancer cells. Urology 80, 1391.e1.
Thomas, C., Tulin, A.V., 2013. Poly-ADP-ribose polymerase: machinery for nuclear processes. Mol. Asp. Med. 34, 1124–1137.
Thomas, C., Kotova, E., Andrake, M., Adolf-Bryfogle, J., Glaser, R., Regnard, C., Tulin, A.V., 2014. Kinase-mediated changes in nucleosome conformation trigger chromatin decondensation via poly(ADP-ribosyl)ation. Mol. Cell 53, 831–842.
Tulin, A., 2011. Re-evaluating PARP-1 inhibitor in cancer. Nat. Biotechnol. 29, 1078–1079.
Wahlberg, E., Karlberg, T., Kouznetsova, E., Markova, N., Macchiarulo, A., Thorsell, A.G., Pol, E., Frostell, A., Ekblad, T., Oncu, D., Kull, B., Robertson, G.M., Pellicciari, R., Schuler, H., Weigelt, J., 2012. Family-wide chemical profiling and structural analysis of PARP and tankyrase inhibitors. Nat. Biotechnol. 30, 283–288.